

Journal of Biomedical Optics

BiomedicalOptics.SPIEDigitalLibrary.org

Induction and imaging of photothrombotic stroke in conscious and freely moving rats

Hongyang Lu
Yao Li
Lu Yuan
Hangdao Li
Xiaodan Lu
Shanbao Tong

Induction and imaging of photothrombotic stroke in conscious and freely moving rats

Hongyang Lu,^{a,b} Yao Li,^{a,b} Lu Yuan,^b Hangdao Li,^b Xiaodan Lu,^b and Shanbao Tong^{a,b,*}

^aShanghai Jiao Tong University, School of Biomedical Engineering, 800 Dongchuan Road, Shanghai 200240, China

^bShanghai Jiao Tong University, Med-X Research Institute, 1954 Huashan Road, Shanghai 200030, China

Abstract. In experimental stroke research, anesthesia is common and serves as a major reason for translational failure. Real-time cerebral blood flow (CBF) monitoring during stroke onset can provide important information for the prediction of brain injury; however, this is difficult to achieve in clinical practice due to various technical problems. We created a photothrombotic focal ischemic stroke model utilizing our self-developed miniature headstage in conscious and freely moving rats. In this model, a high spatiotemporal resolution imager using laser speckle contrast imaging technology was integrated to acquire real-time two-dimensional CBF information during thrombosis. The feasibility, stability, and reliability of the system were tested in terms of CBF, behavior, and T2-weighted magnetic resonance imaging (MRI) findings. After completion of occlusion, the CBF in the targeted cortex of the stroke group was reduced to $16 \pm 9\%$ of the baseline value. The mean infarct volume measured by MRI 24 h postmodeling was $77 \pm 11 \text{ mm}^3$ and correlated well with CBF ($R^2 = 0.74$). This rodent model of focal cerebral ischemia and real-time blood flow imaging opens the possibility of performing various fundamental and translational studies on stroke without the influence of anesthetics. © 2014 Society of Photo-Optical Instrumentation Engineers (SPIE) [DOI: [10.1117/1.JBO.19.9.096013](https://doi.org/10.1117/1.JBO.19.9.096013)]

Keywords: stroke model; laser speckle contrast imaging; cerebral blood flow; freely moving animal; photothrombosis.

Paper 140367R received Jun. 15, 2014; revised manuscript received Aug. 26, 2014; accepted for publication Aug. 28, 2014; published online Sep. 19, 2014.

1 Introduction

Stroke occurs when a cerebral vessel is either blocked or hemorrhagic. Ischemia in the brain can initiate sequential metabolic and biochemical disorders, and subsequently leads to neuronal apoptosis and necrosis.¹ Thus far, almost all laboratory and pre-clinical studies on the topic have been based on animal models of stroke,²⁻⁴ including both global and focal cerebral ischemia models.

Although animal models of ischemic stroke share many similarities with humans in terms of the pathophysiological processes,⁴ many therapeutic strategies that have been successful in animal models have not succeeded in humans, owing to many challenges in bench-to-bedside translation.⁵ The use of anesthetics serves as one major reason for this translational failure, since very few cases of clinical stroke occur under anesthetized conditions.^{6,7} Moreover, a number of animal studies have shown that the administration of anesthetics introduces marked influences on cerebral hemodynamics, cerebral metabolism, cellular and molecular processes, and neural activities, which could lead to neuroprotective outcomes.⁸⁻¹⁰

Another major challenge in stroke studies is the lack of a real-time full-field hemodynamic monitoring methodology, particularly in the acute stage immediately after the onset of stroke. Both experimental and clinical studies have indicated that the early hours after a stroke are the most critical window for therapeutic interventions.^{1,11,12} Moreover, neuroimaging and electro-neurophysiologic studies have demonstrated great prognostic values of early neurovascular changes after stroke.^{13,14} Nevertheless, it is difficult to achieve real-time intraoperative

cerebral blood flow (CBF) monitoring with high spatiotemporal resolution throughout stroke modeling. In the few studies in which stroke has been induced in conscious animals, real-time intraoperative CBF monitoring could not be performed^{15,16} due to various technical problems, such as the interferences introduced by surgical operation and the limited mobility of the devices used. In this study, we report on a wearable miniature headstage (weight: ~20 g, height: 30 mm) capable of inducing a photothrombotic model of focal cerebral ischemia in conscious and freely moving rats. A high spatiotemporal resolution imager was integrated into the headstage for real-time CBF monitoring using laser speckle contrast imaging (LSCI) during and after the stroke modeling. Such a system allows various fundamental and translational studies on stroke to be performed without the influence of anesthetics.

2 Materials and Methods

2.1 Cranial Headstage Setup for Photothrombotic Stroke Modeling

This photothrombotic model of focal cerebral ischemia in conscious and freely moving animals was inspired by our recent miniature head-mounted CBF imager for rodents¹⁷ [Figs. 1(a) and 1(b)]. To induce thrombosis, a single-mode optical fiber (modified from P1-460B-FC-1, Thorlabs, Newton, New Jersey) with an aspheric lens was fixed onto the frame of the headstage to deliver a 532-nm laser beam, with a focus diameter of ~750 μm and power of 5 mW/mm^2 irradiation covering the selected distal middle cerebral artery (MCA).¹⁸⁻²¹ The focus of illumination could be adjusted by driving the anchor screws

*Address all correspondence to: Shanbao Tong, E-mail: shanbao.tong@gmail.com

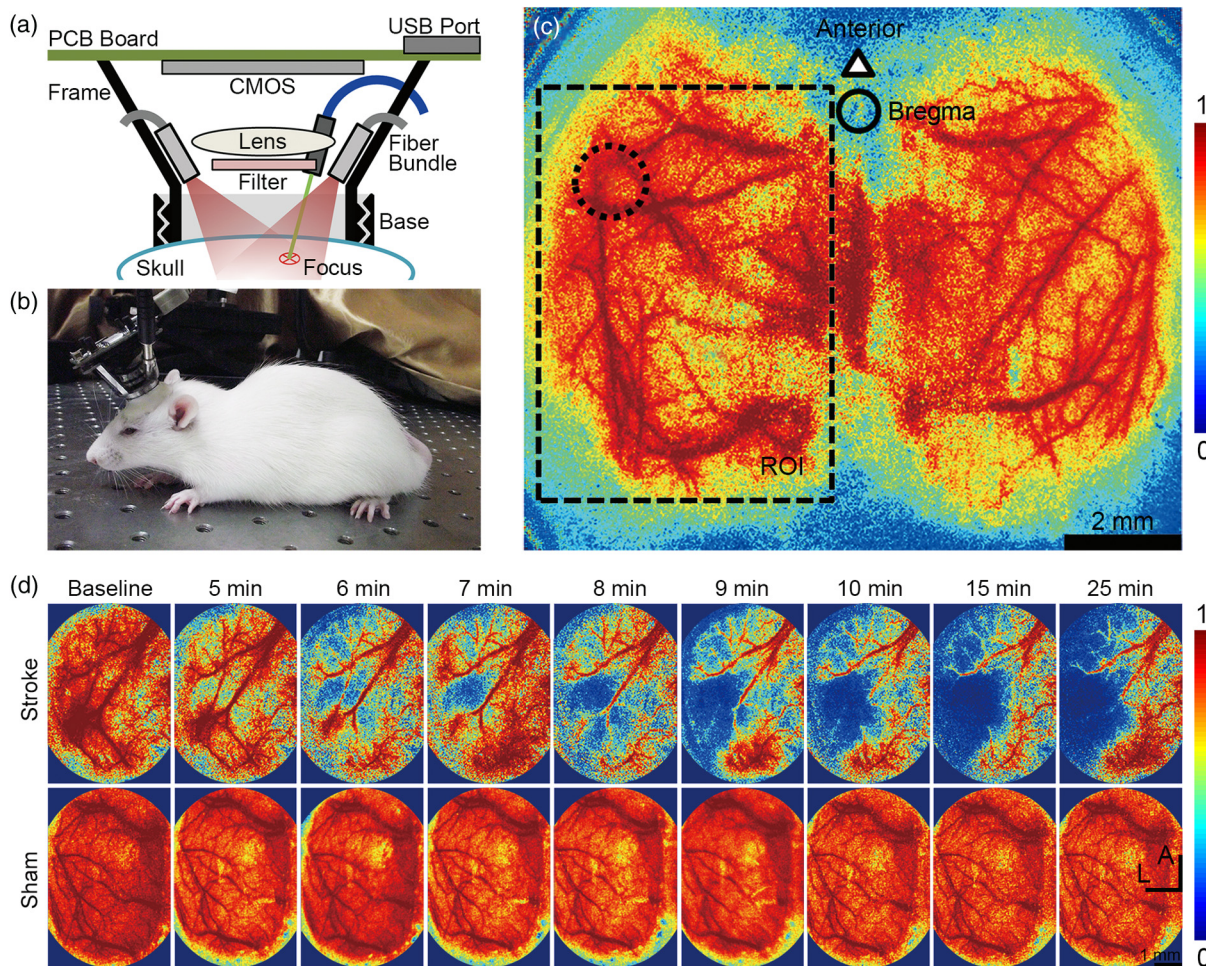


Fig. 1 Overview of the headstage for inducing photothrombotic stroke in conscious and freely moving rats. (a) Schematic of the design. (b) A snapshot of the headstage mounted onto a conscious rat (Video 1, MOV, 1.0 MB) [URL: <http://dx.doi.org/10.1117/1.JBO.19.9.096013.1>]. (c) A typical laser speckle contrast image from a freely moving rat. Dashed circle indicates the 532-nm light focus. A region of interest (ROI) in each rat is selected for further analysis. (d) Cerebral blood flow (CBF) information in ROI before (baseline) and 5 to 10, 15, and 25 min after illumination initiation (Video 2, MOV, 3.1 MB) [URL: <http://dx.doi.org/10.1117/1.JBO.19.9.096013.2>].

so that the ischemic core would be consistent in all animals. The whole headstage consisted of the following components: (1) a supporting frame that could be attached to a cylinder base (laboratory-designed, height: 4.2 mm, radius: 5.5 mm, thickness: 0.5 mm) via a screw connection; (2) a multimodal optical fiber bundle (50 fibers, diameter: 0.25 mm, 0.45 NA) connected to a 780-nm laser beam (L780P010, Thorlabs) as the light source for CBF monitoring; (3) a CMOS sensor (DCC1645M, Thorlabs) on a printed circuit board with a micro-lens system (radius: 3.44 mm, focal length: 5.05 mm, minimum focus distance: 20.00 mm, 0.011 NA) and an optical filter (FGL665, Thorlabs) for blood flow imaging; and (4) a single-mode optical fiber connected to a 532-nm laser beam for inducing ischemia. After injection of photosensitizing dye (Rose Bengal in this study), thrombosis could be induced within 15 min of illumination.

2.2 Cranial Window Preparation

The experimental protocols were approved by the institutional Animal Care and Use Committee of Med-X Research Institute, Shanghai Jiao Tong University. Twenty male Sprague-Dawley

rats (320 ± 20 g, 12 weeks old; Slac Laboratory Animal, Shanghai, China) were used in this study. The rats were housed in a research animal facility and maintained in a comfortable temperature (21 to 25°C) and humidity (20 to 50%) environment, and placed under a 12-h reverse light/dark cycle with free access to food and water. A cranial window was prepared 24 h before stroke modeling. During the preparation, the rats were anesthetized with isoflurane (5.0% initial and 1.0 to 1.5% for maintenance). During the surgery, the animals were constrained in a stereotaxic frame (Benchmark Deluxe™, MyNeuroLab.com, St. Louis, Missouri). Rectal temperature was monitored and maintained at $37.0 \pm 0.2^\circ\text{C}$ with a heating pad and a direct current (DC) control module (FHC Inc., Bowdoin, Maine). A midline incision was made over the scalp and the exposed tissues were cleaned with a scalpel to expose the surface of the skull. A 5.0 mm(horizontal) \times 7.0 mm(vertical) area centered at 3.5 mm posterior and 2.5 mm lateral to the bregma over the left hemisphere was thinned by a high-speed dental drill (Fine Science Tools Inc., North Vancouver, Canada) until the cortical vessels were clearly visible. The cylinder base enclosing the thinned area was fixed onto the skull with reinforced glass ionomer cements (Dental Materials Factory of Shanghai

Medical Instruments Co., Shanghai, China). All procedures were performed under standard sterile precautions. After the cement hardened, animals were caged with sufficient food and water supply for 24 h to eliminate the influences of the anesthetics.

2.3 Photothrombotic Modeling of Focal Cerebral Ischemia

After being caged for 24 h, all rats were briefly constrained to connect the headstage to the cylinder base. The animal was then moved into an open plastic round pail (depth: 0.45 m, diameter: 0.64 m) for the photothrombotic stroke experiment. The headstage could be worn by the rat for up to 120 min without hitting the inner surface or other objects. The rats were randomly divided into the stroke group ($n = 12$) illuminated at the selected location of the MCA after intravenous injection of Rose Bengal dye (80 mg/kg, Sigma-Aldrich Co. LLC., St. Louis, Missouri) into the tail vein and the sham group ($n = 8$), which received a saline injection before receiving illumination. The 532-nm laser beam was focused at the Y-shaped juncture of the frontal and parietal branches of the distal MCA [Fig. 1(c)], a region that has been widely used in previous animal model-based studies. Ischemia was induced by photoactivation of the preinjected Rose Bengal to induce damage to the endothelial cell membranes, which then consequentially results in platelet aggregation and vascular thrombosis.^{22,23}

2.4 Real-Time CBF Monitoring

Laser speckle images could be continuously acquired after connecting the headstage to the cylinder base. Raw images (640×640 pixels) were acquired at 50 fps (exposure time: 5 ms). All image processing algorithms were implemented using MATLAB® software (version 8.1, Mathworks, Natick, Massachusetts). When the animals were freely moving, the motion artifacts could be successfully removed by the online registration laser speckle contrast analysis algorithm.²⁴ After registration, a random process estimator was implemented to obtain the CBF information²⁵ [Fig. 1(d)]. The relative CBF (rCBF) velocity changes in the selected regions of interest could be easily acquired throughout the experiment. The rCBF changes in the MCA were computed to confirm the success of the stroke induction. Moreover, we also acquired the mean rCBF velocity changes in a circular region centered at the illumination focus (diameter: 2.0 mm). To test the reliability of the headstage, we pinpointed and plotted the illumination focus in each rat according to the pixels with the largest CBF decrease at 15 min after illumination initiation (Fig. 2).

2.5 Ethical Evaluation

Physiological parameters before and 3 h after the occlusion were measured while the rats were conscious (BP-98A, Softron, Beijing, China). As an indicator of food intake, the body weight of the rats was monitored before and 24 h after occlusion. Furthermore, following the guidelines by Zimmermann²⁶ and others,^{27,28} three experienced examiners performed independent behavioral assessments throughout the experiments to evaluate the possible experimental pain.

2.6 Validation of Photothrombotic Modeling

The neurological severity score (NSS) was examined in all animals before (baseline) and 24 h after onset of ischemia by three

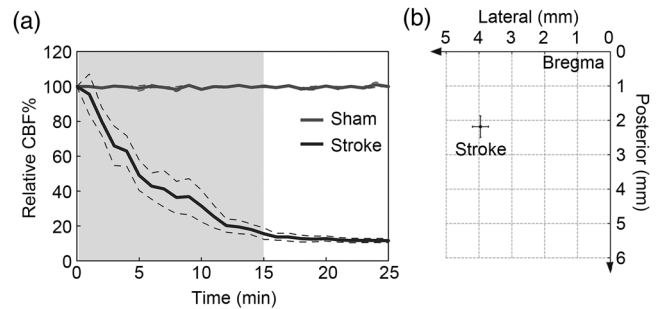


Fig. 2 Reliability of stroke modeling and real-time CBF monitoring. (a) Relative CBF in the middle cerebral artery during the stroke modeling. Dashed lines represent the boundaries of standard deviation. (b) Schematic representation showing the locations of occlusion.

experienced independent examiners were blind to the experimental groups. The NSS is presented as the mean of the examiners' evaluation, scaling from 0 to 18 (normal: 0, maximal deficit score: 18, see Table 1), as previously described by Chen et al.²⁹

T2-weighted magnetic resonance imaging (MRI) was performed 24 h after ischemia onset. The animals were placed in an MRI scanner (Siemens MAGNETOM Trio 3T, Munich, Germany) equipped with a dedicated solenoid rat coil (diameter: 60 mm). The coil was tuned and matched manually. High-resolution T2-weighted spin-echo imaging was used to map the lesion. Twenty continuous coronal slices (thickness: 1 mm) and 20 continuous transversal slices (thickness: 1 mm) were acquired with a field of view of 50×50 mm and a matrix size of 512×512 (repetition time: 3000 ms, echo time: 68 ms, imaging time: 4 min, 2 averages). The total scanning time was ~8 min for each rat. Computer-aided planimetric assessment of the lesion volumes was performed using National Institutes of Health Image software ImageJ (version 1.44).³⁰ After adjustment of contrast, the contours of the hemispheres were traced manually on each slice. The infarct area was calculated manually by the trapezoidal rule, and infarct volume was subsequently calculated by multiplying the infarct area on each slice by the distance between the slices.

2.7 Statistical Analysis

Differences across the groups in terms of the ethical assessment, rCBF, NSS, and infarct volume from MRI were determined by the two-tailed student's t test using MATLAB® software. Significance was set at $p < 0.05$, and all data are expressed as mean \pm SD.

Table 1 Neurological severity scores (modified from Chen et al.²⁹). For each category of assessment, higher score indicates more severe injury.

Motor tests	6
Sensory tests	2
Beam balance tests	6
Reflexes absent and abnormal movements	4
Maximum points	18

Table 2 Vital data acquired before and 3 h after stroke modeling.

		Heart rate (bpm)			Blood pressure (mmHg)		
		Before	After	<i>p</i> value	Before	After	<i>p</i> value
Sham	(<i>n</i> = 8)	355 ± 20	337 ± 35	0.16	105 ± 15	102 ± 18	0.55
Stroke	(<i>n</i> = 12)	352 ± 19	348 ± 21	0.15	103 ± 12	108 ± 10	0.26

Note: Values are expressed as mean ± SD. *p* values are determined by the two-tailed student's *t* test. There are no significant changes in either heart rate or blood pressure after occlusion in either group.

3 Results

3.1 Vital Parameters and Ethical Evaluation

The examined physiological variables are shown in Table 2. For all rats, no significant changes in the heart rate or blood pressure were observed throughout the experiment ($p > 0.05$). Twenty-four hours after occlusion, the body weight losses were $16 \pm 4\%$ and $18 \pm 5\%$ in the stroke and sham groups, respectively ($p > 0.05$), indicating that the modeling did not significantly influence the animals' food intake. No significant painful symptoms, such as provoked behavior, persistent hunching behavior, labored respiration, convulsions, or prostration, were observed during the stroke modeling, indicating that the modeling did not result in noticeable stress or pain. No deaths occurred in either group.

3.2 Real-Time CBF Monitoring

CBF imaging confirmed that the MCAs of all rats in the stroke group were completely occluded by an intraluminal thrombus formed by 532-nm laser illumination within 15 min after Rose Bengal injection [Fig. 2(a)]. Meanwhile, the rats in the sham group did not show significant CBF changes. In the stroke group, the CBF at the distal MCA and the surrounding area decreased to $15.66 \pm 9.17\%$ and $20.14 \pm 7.64\%$ of the baseline values, respectively, after 15-min illumination and remained stable thereafter. All CBF changes are expressed as a percentage of the baseline value. The occlusions aggregated well in the stroke group [3.956 ± 0.244 mm and 2.836 ± 0.441 mm lateral and

posterior to the bregma, respectively, Fig. 2(b)], and the lesion cores indicated good reliability of the stroke modeling.

3.3 Validation of Stroke Modeling

In the stroke group, the NSS was 6.0 ± 1.0 , which was significantly higher than the NSS in the sham group [$p < 0.01$, Fig. 3(a)]. In this study, the NSS was lower than that reported in other rat stroke models, which could be due to the limited infarct volumes in the photothrombotic model.

T2-weighted MRI consistently demonstrated occlusion in the stroke group [Figs. 3(b) and 3(c)]. The mean ischemic lesion volume was significantly higher in the stroke group (77.38 ± 11.09 mm³) compared with the sham group, in which no evident lesions were observed ($p < 0.01$).

Next, a threshold of CBF velocity reduction, 50% of the baseline, was used to determine the occlusion-affected area at the end of illumination. The threshold was determined based on our previous work,¹⁴ in which we found that the area with 50% CBF velocity drop during stroke modeling was closely correlated with the infarct volume at 24 h after stroke. If the CBF reduction area was calculated by the pixels with CBF below the threshold, it showed good correlation with the ischemic lesion volume [$R^2 = 0.74$, Fig. 4(a)]. Furthermore, as shown in Fig. 4(b), the CBF map aligned well with the lesion location in T2-weighted MRI. These data confirmed the reliable mild ischemic brain injury induced by photothrombosis.

4 Discussion

In this study, we designed a miniature headstage that could induce photothrombosis at a target cortex and performed real-time CBF imaging during stroke modeling in conscious and freely moving rats. Compared with other rodent models of focal ischemic stroke, this photothrombotic model has the advantages of minimal invasiveness, stable and controllable lesion volume, and selectable lesion location by tuning the focus of the light illumination. These advantages make this model suitable for

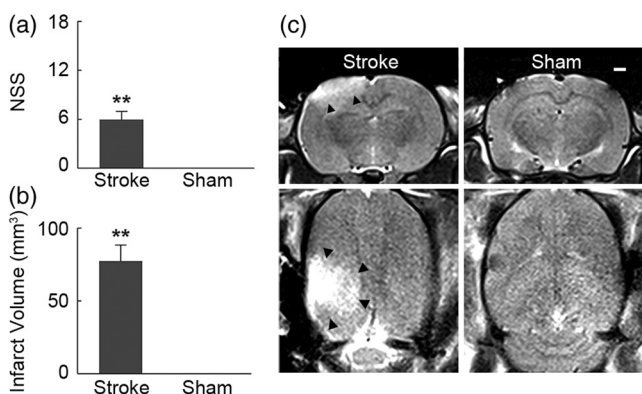


Fig. 3 Validation of stroke modeling. (a) and (b) The neurological severity score and infarct volume in the sham and stroke groups 24 h after occlusion. Data are illustrated in mean ± SD. ** $p < 0.01$. (c) Coronal and transversal planes of T2-weighted magnetic resonance imaging (MRI) 24 h after occlusion reveal a lesion in a stroke rat. No lesion was observed in the sham group. Scale bar, 1 mm.

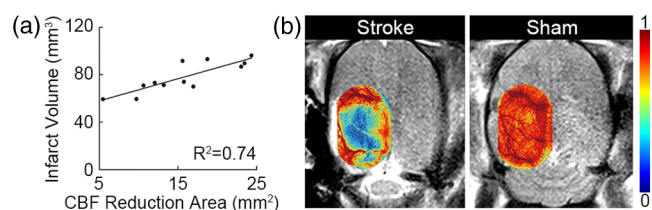


Fig. 4 (a) Correlation between infarct volume 24 h after occlusion and CBF reduction area 15 min after illumination initiation. (b) T2-weighted MRI from one rat overlaid by CBF information 15 min after illumination initiation.

inducing stroke in freely moving animals without anesthesia administration. The whole system introduced negligible incidence of mortality.

By combining this model with LSCI technology, we were able to monitor the CBF changes throughout the induction of thrombosis in real time. By tuning the illumination focus of the 532-nm laser beam, occlusion could be induced at arbitrary selected locations along the distal MCA. This headstage system could also be readily integrated with other optical imaging techniques, such as optical intrinsic signal³¹ and voltage-sensitive dyes,³² to obtain additional neurovascular and hemodynamic information during stroke. Furthermore, by improving the precision of the laser beam, this system can be configured to target a single vessel to create MCA occlusion, which is currently the most commonly used stroke model.³³ We may also induce a reperfusion model of stroke using this system by integrating a pulsed, low-energy-density 351-nm XeF or 248-nm KrF ultraviolet laser to dilate and recanalize the occluded MCA after photothrombosis.²⁰ Further, if we delicately control the illumination intensity and implement chronic optical access through a polished and reinforced thinned skull,³⁴ we may be able to create a chronic cerebral ischemia model in a freely moving animal.

5 Conclusion

In conclusion, we here reported on a wearable miniature headstage capable of inducing a photothrombotic stroke model in conscious and freely moving rats. This model was associated with minor invasiveness and complied with the ethics of animal care and use. Meanwhile, real-time CBF imaging was performed with high spatiotemporal resolution during the modeling using LSCI technology, and the feasibility, stability, and reliability of the system were tested in the aspects of CBF, animal behavior, and MRI findings. This rodent model of focal cerebral ischemia and the use of real-time blood flow imaging open the possibility of performing a variety of fundamental and translational research in stroke without the influence of anesthetics.

Acknowledgments

This work was funded by National Natural Science Foundation of China numbers 81071192, 61371018, and 61102021. The authors are also grateful to Dr. Guo-Yuan Yang for helpful discussions on animal experiments.

References

1. E. H. Lo, T. Dalkara, and M. A. Moskowitz, "Mechanisms, challenges and opportunities in stroke," *Nat. Rev. Neurosci.* **4**(5), 399–415 (2003).
2. M. D. Ginsberg and R. Busto, "Rodent models of cerebral ischemia," *Stroke* **20**(12), 1627–1642 (1989).
3. U. Dirnagl, C. Iadecola, and M. A. Moskowitz, "Pathobiology of ischemic stroke: an integrated view," *Trends Neurosci.* **22**(9), 391–397 (1999).
4. S. T. Carmichael, "Rodent models of focal stroke: size, mechanism, and purpose," *NeuroRx* **2**(3), 396–409 (2005).
5. U. Dirnagl, "Bench to bedside: the quest for quality in experimental stroke research," *J. Cereb. Blood Flow Metab.* **26**(12), 1465–1478 (2006).
6. D. J. Gladstone et al., "Toward wisdom from failure: lessons from neuroprotective stroke trials and new therapeutic directions," *Stroke* **33**(8), 2123–2136 (2002).
7. M. Fisher and T. Tatlisumak, "Use of animal models has not contributed to development of acute stroke therapies con," *Stroke* **36**(10), 2324–2325 (2005).
8. A. W. Gelb et al., "Propofol anesthesia compared to awake reduces infarct size in rats," *Anesthesiology* **96**(5), 1183–1190 (2002).
9. H. Kitano et al., "Inhalational anesthetics as neuroprotectants or chemical preconditioning agents in ischemic brain," *J. Cereb. Blood Flow Metab.* **27**(6), 1108–1128 (2006).
10. C. Martin et al., "Investigating neural-hemodynamic coupling and the hemodynamic response function in the awake rat," *Neuroimage* **32**(1), 33–48 (2006).
11. T. H. Murphy and D. Corbett, "Plasticity during stroke recovery: from synapse to behaviour," *Nat. Rev. Neurosci.* **10**(12), 861–872 (2009).
12. W. Hacke et al., "Association of outcome with early stroke treatment: pooled analysis of ATLANTIS, ECASS, and NINDS rt-PA stroke trials," *Lancet* **363**(9411), 768–774 (2004).
13. N. Hjort et al., "Ischemic injury detected by diffusion imaging 11 minutes after stroke," *Ann. Neurol.* **58**(3), 462–465 (2005).
14. Y. Li et al., "Predicting the ischemic infarct volume at the first minute after occlusion in rodent stroke model by laser speckle imaging of cerebral blood flow," *J. Biomed. Opt.* **18**(7), 076024 (2013).
15. A. Seto et al., "Induction of ischemic stroke in awake freely moving mice reveals that isoflurane anesthesia can mask the benefits of a neuroprotection therapy," *Front. Neuroenergetics* **6**, 1 (2014).
16. R. Liu et al., "Extendable, miniaturized multi-modal optical imaging system: cortical hemodynamic observation in freely moving animals," *Opt. Express* **21**(2), 1911–1924 (2013).
17. P. Miao et al., "Laser speckle contrast imaging of cerebral blood flow in freely moving animals," *J. Biomed. Opt.* **16**(9), 090502 (2011).
18. R. Prado et al., "L-arginine does not improve cortical perfusion or histopathological outcome in spontaneously hypertensive rats subjected to distal middle cerebral artery photothrombotic occlusion," *J. Cereb. Blood Flow Metab.* **16**(4), 612–622 (1996).
19. B. D. Watson et al., "Argon laser-induced arterial photothrombosis. Characterization and possible application to therapy of arteriovenous malformations," *J. Neurosurg.* **66**(5), 748–754 (1987).
20. B. D. Watson et al., "Cerebral blood flow restoration and reperfusion injury after ultraviolet laser-facilitated middle cerebral artery recanalization in rat thrombotic stroke," *Stroke* **33**(2), 428–434 (2002).
21. C. G. Markgraf et al., "Comparative histopathologic consequences of photothrombotic occlusion of the distal middle cerebral artery in Sprague-Dawley and Wistar rats," *Stroke* **24**(2), 286–292 (1993).
22. W. I. Rosenblum and F. El-Sabban, "Platelet aggregation in the cerebral microcirculation: effect of aspirin and other agents," *Circ. Res.* **40**(3), 320–328 (1977).
23. B. D. Watson et al., "Induction of reproducible brain infarction by photochemically initiated thrombosis," *Ann. Neurol.* **17**(5), 497–504 (1985).
24. P. Miao et al., "High resolution cerebral blood flow imaging by registered laser speckle contrast analysis," *IEEE Trans. Biomed. Eng.* **57**(5), 1152–1157 (2010).
25. P. Miao et al., "Random process estimator for laser speckle imaging of cerebral blood flow," *Opt. Express* **18**(1), 218–236 (2010).
26. M. Zimmermann, "Ethical guidelines for investigations of experimental pain in conscious animals," *Pain* **16**(2), 109–110 (1983).
27. H. Brugere et al., "Pain and distress in laboratory rodents and lagomorphs," *Lab. Anim.* **28**(2), 97–112 (1994).
28. P. Hawkins, "Recognizing and assessing pain, suffering and distress in laboratory animals: a survey of current practice in the UK with recommendations," *Lab. Anim.* **36**(4), 378–395 (2002).
29. J. Chen et al., "Therapeutic benefit of intravenous administration of bone marrow stromal cells after cerebral ischemia in rats," *Stroke* **32**(4), 1005–1011 (2001).
30. C. A. Schneider, W. S. Rasband, and K. W. Eliceiri, "NIH image to ImageJ: 25 years of image analysis," *Nat. Methods* **9**(7), 671–675 (2012).
31. A. Grinvald et al., "Functional architecture of cortex revealed by optical imaging of intrinsic signals," *Nature* **324**(6095), 361–364 (1986).
32. G. G. Blasdel and G. Salama, "Voltage-sensitive dyes reveal a modular organization in monkey striate cortex," *Nature* **321**(6070), 579–585 (1986).
33. H. Yao et al., "Reperfusion-induced temporary appearance of therapeutic window in penumbra after 2 h of photothrombotic middle cerebral artery occlusion in rats," *J. Cereb. Blood Flow Metab.* **29**(3), 565–574 (2009).
34. P. J. Drew et al., "Chronic optical access through a polished and reinforced thinned skull," *Nat. Methods* **7**(12), 981–984 (2010).

Hongyang Lu received his BS degree in biomedical engineering from Shanghai Jiao Tong University in 2010, where he is currently working toward his PhD degree in biomedical engineering. His current research interests include functional neuroimaging and therapeutic strategies on brain injury. He is a student member of the Institute of Electrical and Electronics Engineers (IEEE). He also has been a visiting student researcher at Johns Hopkins University School of Medicine since January 2014.

Yao Li received her BS degree from Shanghai Jiao Tong University in 2002 and her PhD degree from the State University of New York at Stony Brook in 2008. She then joined Stony Brook Medical Center as a senior postdoctoral associate. She is a member of IEEE and the Organization of Human Brain Mapping. She joined Med-X Research Institute in 2010 as an associate professor.

Lu Yuan received her BS degree from Shanghai Jiao Tong University in 2012. She is a master's student at Shanghai Jiao Tong University. Her research interests include laser speckle imaging and surgical technique of rodent stroke models.

Hangdao Li received his BS and MS in biomedical engineering from Shanghai Jiao Tong University in 2011 and 2013. Currently, he is a second-year PhD student at the Shanghai Jiao Tong University, focusing on studies of optical imaging and transcranial ultrasound stimulation.

Xiaodan Lu is a graduate student in the Neural Engineering Laboratory, School of Biomedical Engineering, Shanghai Jiao Tong University. Her research mainly focuses on optical imaging of the cerebral cortex, including laser speckle imaging and optical coherence tomography, and the study of stroke based on those methods in conscious animals.

Shanbao Tong is the director of the Neural Engineering Laboratory, Shanghai Jiao Tong University. He got his BSc in radio technology from Xi'an Jiao Tong University in 1995, an MSc in turbine machines, and a PhD in biomedical engineering from Shanghai Jiao Tong University in 1998 and 2002, respectively. His research interests include neural signal processing, neurophysiology of brain injury, and cortical optical imaging.